

The onion model, a simple neutral model for the evolution of diversity in bacterial biofilms

J. M. EASTMAN*†, L. J. HARMON*†, H.-J. LA*†, P. JOYCE†‡ & L. J. FORNEY*†

*Department of Biological Sciences, University of Idaho, Moscow, ID, USA

†Initiative for Bioinformatics and Evolutionary Studies (IBEST), University of Idaho, Moscow, ID, USA

‡Departments of Statistics and Mathematics, University of Idaho, Moscow, ID, USA

Keywords:

antibiotic resistance;
Escherichia coli;
insurance effect;
Moran model;
neutral evolution.

Abstract

Bacterial biofilms are particularly resistant to a wide variety of antimicrobial compounds. Their persistence in the face of antibiotic therapies causes significant problems in the treatment of infectious diseases. Seldom have evolutionary processes like genetic drift and mutation been invoked to explain how resistance to antibiotics emerges in biofilms, and we lack a simple and tractable model for the genetic and phenotypic diversification that occurs in bacterial biofilms. Here, we introduce the ‘onion model’, a simple neutral evolutionary model for phenotypic diversification in biofilms. We explore its properties and show that the model produces patterns of diversity that are qualitatively similar to observed patterns of phenotypic diversity in biofilms. We suggest that models like our onion model, which explicitly invoke evolutionary process, are key to understanding biofilm resistance to bactericidal and bacteriostatic agents. Elevated phenotypic variance provides an insurance effect that increases the likelihood that some proportion of the population will be resistant to imposed selective agents and may thus enhance persistence of the biofilm. Accounting for evolutionary change in biofilms will improve our ability to understand and counter diseases that are caused by biofilm persistence.

Introduction

Bacterial biofilms are assemblages of bacterial cells embedded within an extracellular matrix of polymeric compounds. Biofilms are common in the natural world (Battin *et al.*, 2007). The importance of biofilms in the persistence of many infectious diseases is well known (see Lewis 2001, Mah and O’Toole 2001, Stewart & Costerton, 2001, and Hall-Stoodley *et al.* 2004 for reviews). Biofilms are of medical relevance because of their environmental abundance and persistence, but are of particular concern because of their recalcitrance to a wide variety of therapeutic treatments (Stewart & Costerton, 2001; Hall-Stoodley *et al.* 2004).

Biofilms exhibit marked resistance to antibiotics, persist in a variety of challenging environments and show large phenotypic variance. Previous work on the origin and

maintenance of antimicrobial resistance in biofilms has largely focused on three hypotheses (for review, see Stewart & Costerton, 2001 and Hall-Stoodley *et al.*, 2004). First, the extracellular matrix of a biofilm may provide a physical barrier to toxicant diffusion. Under this model, cells most external in biofilms should be most susceptible to antimicrobial toxicity (e.g. Chen & Stewart, 1996; but see Stewart, 1996 and Cochran *et al.*, 2000). Second, the presence of physiologically dormant cells (‘persisters’) is often posited as an explanation for biofilm resistance to antibiotics, and these bacteria reconstitute the biofilm following exposure to antibiotics (e.g. Balaban *et al.*, 2004). These ‘persister’ phenotypes are often attributed to phenotypic plasticity of individual cells, which in turn are described as exhibiting a ‘biofilm phenotype’ (e.g. see Drenkard & Ausubel, 2002; Balaban *et al.*, 2004; Wiuff *et al.*, 2005). Differential gene expression in response to antibiotic treatment is offered as an additional mechanism of plasticity by which isogenetic populations might contribute to the biofilm phenotype (Jothi *et al.*, 2009).

Although current hypotheses of mechanisms for biofilm resistance are varied, evolutionary processes – like

Correspondence: Larry J. Forney, Department of Biological Sciences, University of Idaho, Moscow, ID 83844, USA.
Tel.: +1 208 885 6011; fax: +1 208 885 6280;
e-mail: lforney@uidaho.edu

genetic drift, mutation and selection – are seldom invoked as viable explanations for biofilm resistance to antibiotics. Yet the application of evolutionary modelling to microbial populations is fundamentally an old idea that dates back to at least 1943, when Luria and Delbrück demonstrated that spontaneous mutations underlying variation in pathogen sensitivity can occur readily and in the absence of selection. Although the stochastic nature of mutation is today very well received, this seminal paper overturned a great deal of work positing the sole importance of pathogen-induced variation in bacterial resistance to infection. The role of mutation in development and persistence of phenotypically diverse communities is incontrovertible (e.g. see Boles & Singh, 2008 for an example in *Pseudomonas aeruginosa* biofilms). However, we argue that the stochastic process of mutation has been underappreciated as a cause of extensive phenotypic diversification in biofilms (but see J.G. Tyerman, J. Ponciano, P. Joyce, L.J. Forney & L.J. Harmon, unpublished data; Boles *et al.*, 2004; and Conibear *et al.*, 2009).

Our aim in this study is to model the stochastic processes of bacterial replication and mutation, evaluating the resulting extent and distribution of phenotypic variation within simulated biofilms. Extremely large population size – typical of bacterial biofilms – can enhance total diversity found within populations (Wright, 1931; Kimura, 1983; Kingman, 1982; Charlesworth, 2009). Bacteria also have rapid generation times and high mutation rates under some circumstances (Matic *et al.*, 1997), which may further facilitate the accumulation of total diversity during biofilm growth. If we assume that much phenotypic variation arises through mutation, we ask whether antimicrobial resistance in biofilms can be understood as a consequence of population size, mutability, and spatially structured development of biofilms. If we consider two forms of mutation, occurring at a rate either dependent (μ) or independent (ν) of bacterial replication, we expect that a relative balance in the mutational process should largely determine the spatial distribution of diversity within the biofilm. If replication-independent mutation outstrips replication-dependent mutation (that is, $\nu \gg \mu$), we expect ancestral (lower) layers of the biofilm will have accrued a disproportionately large degree of phenotypic diversity as these layers will have endured for longer periods. By contrast, if $\mu \gg \nu$, the reverse should hold, and we expect ancestral layers to be the most phenotypically depauperate.

Unlike existing models that are often parameter rich (Kreft *et al.*, 1998; Chang *et al.*, 2003), we intentionally narrow the set of assumptions and parameters in our neutral model of biofilm development. In a simulation study, we ask whether the modelled process is sufficient to explain observed patterns of diversity partitioning from *in vitro* biofilms of *Escherichia coli* MG1655 where phenotypic diversity appears highest in the uppermost strata (see Ponciano *et al.*, 2009).

The onion model

1. Successive generations are derived from earlier ones.
2. New layers eventually are buried and become stressed due to nutrient limitation.
3. Cells in emergent layers have many of the mutations of preceding generations.
4. Cells in deeper layers are quiescent.

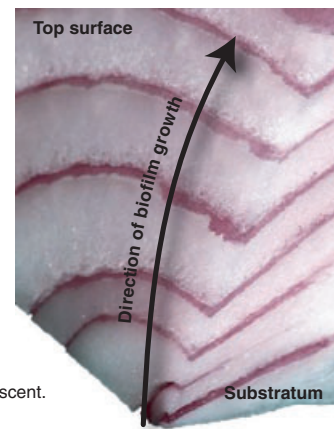


Fig. 1 Laminar growth in the ‘onion model’ as illustrated by a sectioned onion. In the onion model, biofilm growth is initiated by colonization of the substratum by a single cell (lowermost section). Successive generations of cells in a new layer are derived from earlier (and lower) progenitors, and cells in new layers inherit many of the mutations of their progenitors. With continued growth, formerly emergent layers transition into quiescence as new layers restrict growth of the now concealed layers. Quiescent cells – those within internal layers – are assumed to be growth-limited. This transition into quiescence thus acts to fix mutational variants in space.

Methods

Biofilm simulations

We use an individual-based model to simulate biofilm development. The simulated biofilm is a cube, where each side has an equal length in units of cells. Drawing from population genetics, we model growth and change within the simulated biofilm through space and time as a Moran (1962) process. All simulations used a cube volume of 10^6 cells (i.e. 100 cells per side). Beginning each simulation with a single organism, the biofilm space is progressively filled one cell at a time. If a space within the cube is occupied by an individual, the individual may mutate, die or remain unchanged. If the space is empty, replication may populate the space with a descendant whose ancestor was one of the nearest neighbours, from either the same layer or the first layer beneath (with a further restriction discussed below). For an internal position, each cell has eight nearest neighbours in the same layer, with four cells adjacent and four cells from each diagonal. For simulations described herein, we assume that the death rate is negligible and that the accretion of additional layers in the biofilm does not happen until the nearest underlying layer of the simulated biofilm is fully populated. This manner of laminar growth we refer to as the ‘onion model’¹ (Fig. 1).

¹It should be noted that actual onions do not truly grow in this manner but instead develop with the youngest layers towards the centre of the bulb.

Under our simulated onion model, lateral and vertical growth in the biofilm growth are governed differently. In particular, lateral growth considers neighbouring occupants within same layer as well occupants in the antecedent layer. We can describe growth of the biofilm by considering, for each cell in a biofilm, the 17 immediate neighbouring positions at or below the considered cell: nine in the layer below and eight in the same layer. If the positions of nearest neighbours in the lower layer are populated, local replication necessarily ensues to populate the empty element. Where more than the necessary nine (lower) positions are occupied, either lateral or vertical growth may occur. The probability of occupation from a given variant is given by its local abundance. Initiation of growth into a subsequent layer occurs only if the present layer is fully populated. Vertical and lateral growth thus emerge naturally from the onion model at a global rate governed by the shape of the simulated biofilm and the employed assumption of nearest-neighbour local growth. We terminate simulations when every cell in the predefined biofilm space becomes occupied. A generation is here defined as the minimum period required for population doubling.

Two forms of selectively neutral mutation were modelled; these mutabilities are the two primary parameters on which we focus. First, we consider mutation in the standard population genetic manner: mutations occur at some rate per individual per replication event (μ). Second, by assuming that mutability may depend on the physiological state of the bacterium, we consider a secondary rate of mutation for physiologically quiescent (nonreplicating) cells (ν). Both mutation rates are stochastically constant. Processes encompassed by ν include stress-induced mutagenesis, which may underlie much of the mutational intensity in natural populations (Bjedov *et al.*, 2003; Galhardo *et al.*, 2007). We consider two independent phenotypic traits in our simulations, treating each as if they evolve with perfect heritability. First, we evolve (i) a continuous trait by a random walk (see Felsenstein, 1973); each phenotypic mutation is normally distributed around the ancestral phenotypic value, $N \sim (0, 0.01)$. Second, we evolve (ii) a categorical trait within an infinite allele framework (Kimura & Crow, 1964) in which every mutational perturbation forms a measurably unique phenotype. In this case, the phenotypic distance between one variant and any other is equivalent.

To parameterize our simulation conditions, we require a pair of independent rates for μ and ν . We consider five mutational intensity (m), ranging from 10^{-5} , 10^{-4} , ..., 10^{-1} and where $m = \mu + \nu$. For each mutational intensity, we consider the relative balance between μ and ν as an important diversification parameter. Our measure of balance in the mutational process (s) is $(\mu - \nu)/(\mu + \nu)$ and ranges between -1 and 1 . Values nearer to -1 reflect a mutational process overwhelmed by ν . We choose nine equally spaced mutational balances ($-1, -3/4, \dots, 1$). We conduct nine replicate simulations for all combinations of

μ and ν . We thus investigate 45 mutational combinations, for a total of 405 simulations.

Growth-structuring simulations

To directly study the effect of structured growth on diversification, we conducted a second set of simulations for which bacterial growth was consistent either with the onion model (Fig. 1) or with planktonic culture. Simulated growth in planktonic populations is unstructured and is intended to model diversification in a well-mixed culture. Replication that populates a currently unpopulated space in the planktonic population is spatially unrestricted: any living individual is as likely as any other to be the progenitor. All evolutionary aspects of planktonic diversification are in accord with simulations conducted under the onion model of biofilm growth (see Biofilm Simulations). We use four (maximal) population sizes to compare diversification between these two models of growth. Simulations consider a range of population sizes between 8^3 , 16^3 , 32^3 or 64^3 cells, and we terminate simulations when these maximal population sizes are reached. We consider a range of m (10^{-4} , 10^{-3} , 10^{-2} , 10^{-1}) and the same range of mutational balances, s , as previously. With 144 parameter combinations for each growth model and nine replicates for each combination, we thus investigate a total of 2592 simulations.

Statistical analyses

All simulations were conducted and analysed using base packages provided in the R 2.13.1 environment (R Development Core Team, 2011). In the first set of *Biofilm Simulations*, we focus our attention on the distribution of phenotypic diversity that arises under a range of mutational conditions (e.g. where ν outstrips μ , where μ outstrips ν and where these rates are balanced). To determine how phenotypes are spatially distributed in the biofilms, we assess biofilm diversity for each layer. Simulated biofilm layers comprise 10^4 total cells in a layer, each of which is 1 cell in depth. For our continuous trait, we measure the average squared difference of each phenotypic value from that of the ancestor (δ^2); for our categorical trait, we use the Gini–Simpson index of diversity (Gini, 1912; Simpson, 1949), which accounts for the relative abundance of each categorical variant in each layer.

We use linear regression to assess diversity stratification through layers of the biofilm. For each simulation, we focus on the fitted slope of regression for biofilm depth (measured from the bottom of the biofilm) on phenotypic diversity (hereafter β_s). A positive slope corresponds to the situation where most of the phenotypic diversity is apportioned towards the uppermost layers of the biofilm, whereas a negative slope indicates that most of the diversity is in layers of biofilm nearest the substratum. To assess the role of the mutational process in biofilm diversification across simulations, we

use the fitted slopes of diversity stratification from individual simulations (β_s) as our response variable. We use multiple regression to evaluate the relative importance of mutational intensity (m) and mutational balance (s) in the observed stratification of phenotypic diversity.

Our primary variable of interest in the set of *growth-structuring simulations* was the average squared deviance of phenotypic values from the ancestral trait value (δ^2) for a neutral continuous trait. We again use multiple regression to assess dependence of this measure of diversification on maximal population size, mutational intensity (m), mutational balance (s), and growth structure (either onion-model biofilm development or planktonic culture).

Results

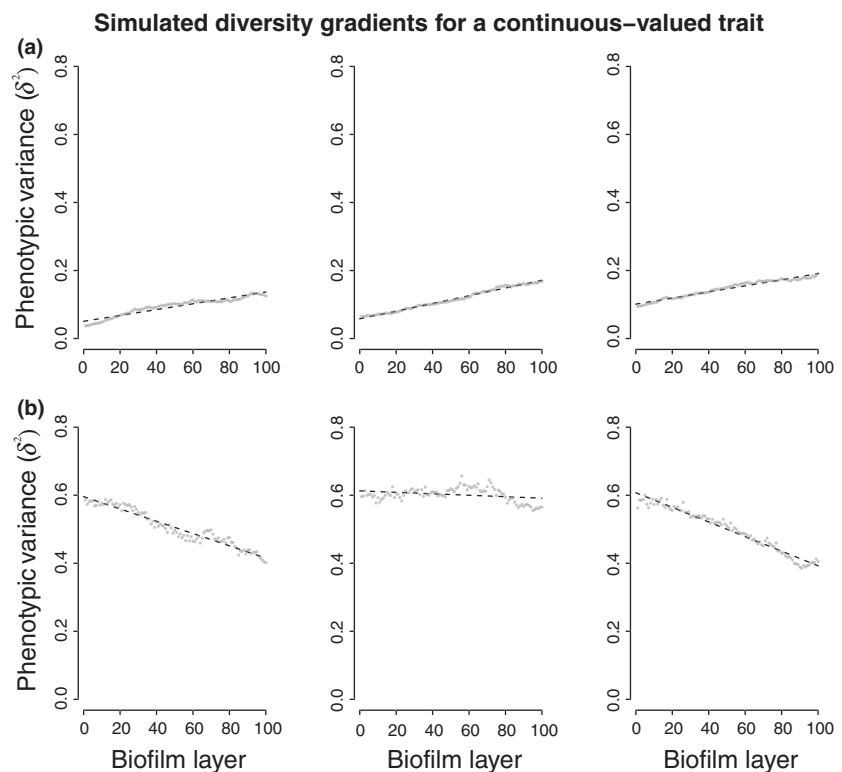
Biofilm simulations

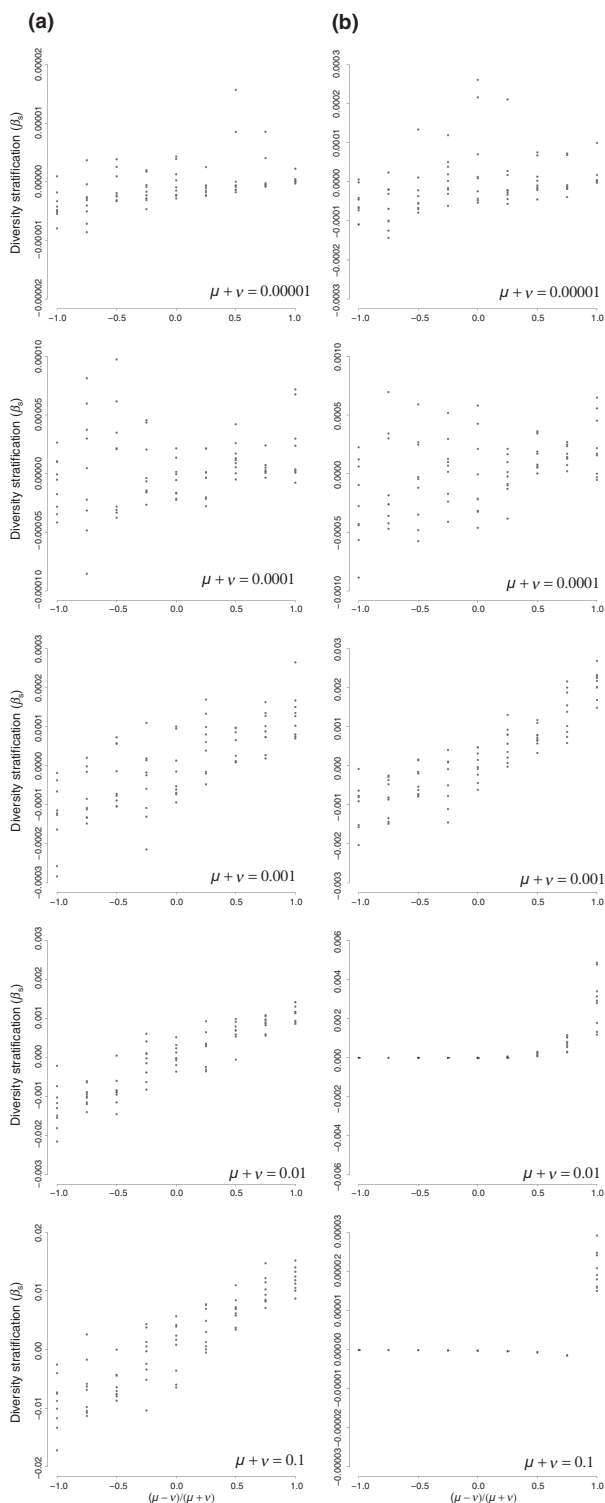
Our simulations show that under simple neutral models, the nature of partitioning of phenotypic diversity in biofilms is strongly dependent upon the balance between mutational processes. In particular, when growth-dependent mutability is in excess of the growth-independent mutation rate, highest phenotypic diversity is often apportioned towards the youngest (uppermost) layers of the biofilm (Fig. 2; Appendix S1).

Results show that in our model, diversity stratification (β_s) is dependent, in part, on the balance between

replication-dependent and replication-independent mutation (Fig. 3; Appendix S1). β_s estimates the relationship between biofilm layer depth and phenotypic diversity for a given simulation (see Methods and Fig. 2). If replication-dependent mutation exceeds replication-independent mutation, we typically witness a significant increase in diversity in layers closest to the leading edge (topmost layer) of biofilm growth under the onion model. For the continuously valued trait simulations, our scaled measure of the mutational dynamic, $s = (\mu - v)/(\mu + v)$, as well as the total mutational supply, $m = \mu + v$, is strongly predictive of patterns in diversity structuring (s : $t_{402} = 10.05$, $P < 0.001$; m : $t_{402} = 2.54$, $P = 0.011$; Fig. 3a). In contrast, only the scaled measure of mutational dynamics is significantly predictive of diversity partitioning of our categorical trait when diversity gradients were assessed with the Gini–Simpson index (s : $t_{402} = 11.53$, $P < 0.001$; m : $t_{402} = -1.76$, $P = 0.079$; Fig. 3b). In simulations with high mutational intensity (e.g. $\mu + v \geq 0.01$) and where mutational intensity exerted by v is exceptionally high, nearly every individual has a unique phenotype and the Gini–Simpson index of diversity approaches 1.0 for each layer in the simulated biofilm (see Appendix S1). Where diversity is saturated, a strong gradient in diversity thus becomes impossible for this bounded estimator of diversity (e.g. lowermost panels of Fig. 3b). In contrast, the estimator of diversity used in Fig. 3a (δ^2) is unbounded, reflecting the extent of divergence from the ancestral

Fig. 2 Results from representative simulations of a continuous trait evolving by random walk under two mutational conditions: (a) three replicates where replication-dependent mutation, μ , is 0.01 and replication-independent mutation, v , is 0.00; (b) three replicates where μ is 0.00 and v is 0.01. Phenotypic variance (δ^2) is the mean sum of square distance from the ancestral phenotypic value within each layer. Biofilm layer corresponds to spatial distance from the ancestral stratum, 0; larger values along the abscissa represent more recently formed strata. Fitted slopes (termed β_s) for the relationship between diversity and depth within the biofilm are used for further statistical analyses. The fitted coefficients of the linear model (including β_s) are shown as dotted lines in each replicate.





phenotype. We thus attribute differences in the lowermost plots of Fig. 3 to boundedness of the two diversity estimators used.

Fig. 3 Patterns in the stratification of phenotypic diversity (β_s) in simulated biofilms, for (a) a continuous trait evolving by a random-walk process and (b) a discontinuous (categorical) trait. Ordinates are fitted slopes of the relationship between diversity and biofilm layer depth for individual simulations (β_s ; see Fig. 2). From top to bottom, plots are split by mutational intensity in simulations ($\mu + \nu$), ranging from 10^{-5} to 10^{-1} . Note the use of unique axis scales for the ordinates in each plot. Where $\beta_s < 0$, most phenotypic diversity is situated towards the ancestral layers of the simulated biofilm; $\beta_s > 0$, most recently formed layers in the simulated biofilm exhibit greatest diversity. More extreme values of β_s thus suggest steeper gradients in biofilm diversity. An interaction between total mutational intensity ($\mu + \nu$) and diversity estimator (comparing panels A to panels B) is readily observed in these plots. The null expectation of no diversity gradient (i.e. $\beta_s = 0$) is indicated by dashed line. (A) Where the mutational process is most highly influenced by replicative mutation (μ), diversity tends to be disproportionately concentrated in the upper layers of the biofilm. Maximal steepness in diversity gradients are directly related to mutational intensity (see Results). (B) Plots show patterns in the stratification of diversity for a discontinuous and polygenic trait where any allele differing from the wild type is considered as phenotypically divergent as any other (see Methods). We use the Gini-Simpson index of diversity in these plots. Similar to panel A, we find a general trend towards steeper diversity gradients where the mutational process is strongly imbalanced between μ and ν , yet we observe a strong nonlinear interaction with mutational intensity (lowermost panels B; see Results).

Growth-structuring simulations

Spatially structured growth contributes to exceptional diversification of simulated biofilm populations (Fig. 4). Whereas per-generation rates of diversification appeared no different between biofilm and planktonic cultures ($t_{2587} = 1.51$, $P = 0.132$), total diversification (δ^2) in simulated populations was strongly dependent on growth structure (Fig. 4; Appendix S2). Biofilm populations on average exhibited ~ 10 -fold greater overall diversity in comparison with planktonic cultures ($t_{2587} = 17.66$, $P < 0.001$; Fig. 4). This result is consistent with elevated variance in antimicrobial resistance observed in biofilm relative to planktonic cultures (e.g. Costerton *et al.*, 1987; Surdeau *et al.*, 2010). As expected, disparity in this contrast between planktonic and biofilm populations is directly related to both population size ($t_{2587} = 15.42$, $P < 0.001$) and mutational intensity ($t_{2587} = 32.07$, $P < 0.001$). Mutational balance (s) is a strong negative correlate of phenotypic diversity ($t_{2587} = -7.81$, $P < 0.001$), and diversity disparity between biofilm and planktonic cultures tends to zero as the mutational process becomes dominated by replicative mutation (Fig. 4).

Discussion

The apparent preadaptation of biofilm populations for antimicrobial resistance lacks a unified explanation. The nature of biofilm antibiotic resistance, as a general

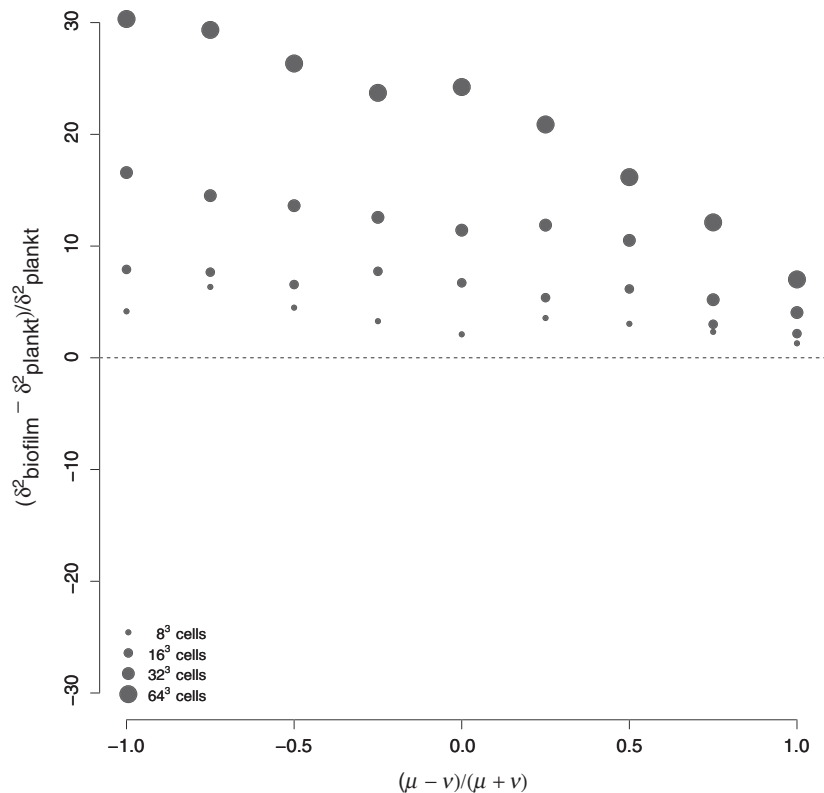


Fig. 4 Patterns in the phenotypic diversification in simulated biofilms vs. simulated 'planktonic' cultures for four maximal population sizes (8^3 , 16^3 , 32^3 or 64^3 cells). Ordinates indicate fold-change in phenotypic diversity comparing biofilm ($\delta^2_{\text{biofilm}}$) to planktonic (δ^2_{plankt}) cultures; each point is the median across 36 paired simulations. Simulated biofilms generally exhibit greater diversity than planktonic populations; the null expectation of no difference in phenotypic variances is indicated by dashed line. The diversity contrast is especially pronounced where the mutational process is most heavily influenced by replicative mutation (ν).

phenomenon, is almost certainly multifarious and may involve heritable variation (J.G. Tyerman *et al.*, unpublished data; Boles *et al.*, 2004; Conibear *et al.*, 2009; for reviews, see Mah & O'Toole 2001 and Hall-Stoodley *et al.* 2004). Our aim here has been to provide expectations in the distribution of heritable variation from a simple model of biofilm growth and diversification. By preventing the occurrence of selective sweeps (or any form of trait-dependent growth), spatial structuring of the onion model preserves a large extent of phenotypic diversity that arises within the biofilm. We expect this elevated diversity to act as an abundant seed bank that can be favourably exploited with the change of environmental conditions, as with antibiotic exposure (Fig. 4; see Yachi & Loreau, 1999 and Boles *et al.*, 2004).

We find strong dependencies in the partitioning of diversity through simulated biofilms, largely as a function of the relative balance between two mutational processes (Fig. 3). Where diversity is primarily generated from a replicative process (i.e. from the contribution of μ ; see Methods), much of the phenotypic variation is distributed within the most recently formed layers of the simulated biofilm (Figs 2–3, 5). Thus, if variation in biofilms accumulates in a manner similar to what we observe here in simulation and if $\mu \gg \nu$, we might predict that a large extent of variance in antibiotic sensitivity is

to be found in the uppermost (youngest) regions of a biofilm. Cells within the youngest layers of the simulated biofilm have greatest generational separation from the original progenitor cell of the biofilm. As such, younger layers thus have greater opportunity to sample from diversity that had arisen by mutation (involving both μ and ν) in each interceding layer. We thus expect (and observe) diversity gradients to be most strongly positive where replicative mutation is the dominant component of mutation (Fig. 3). This result is quite consistent with both theoretical and empirical work on expanding the growth of spatially structured populations (see Hallatschek *et al.*, 2007 and Hallatschek & Nelson, 2010). By contrast, cells that have persisted longer (i.e. those nearest the substratum in the onion model) have greater opportunity to accumulate diversity by nonreplicative mutation (ν). During onion-model growth, descendant layers sample from the *standing* diversity of a progenitor layer, and whereas much of this diversity is retained at the growth front (e.g. Hallatschek & Nelson, 2010), some of the rarer variants must be lost by drift in the emergent layer. We expect these processes to contribute to the concentration in substratal diversity where ν is a dominant component of mutation (Fig. 3).

Our aim was to make predictions based on a simple neutral model, but surely other processes occur and are influential in phenotypic diversification of microbial pop-

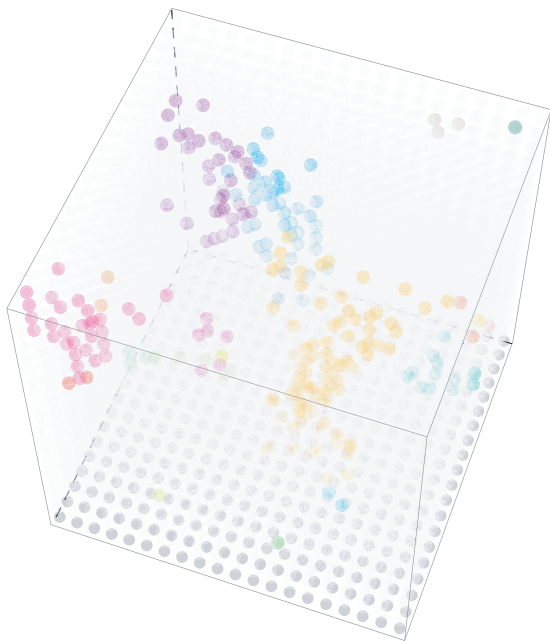


Fig. 5 A schematic representation of a simulated biofilm, where the most visible (uppermost) layer is the youngest. Throughout the biofilm, a multitude of variants (coloured circles), distinct from the ancestral type (very light grey circles), are visible; to aid in orientation, cells in the lowermost (ancestral) layer have been darkened. Cells that are more internal (i.e. closer to the ancestral layer) are lighter in hue. A clonal expansion of a variant coloured blue can be seen left of centre in the cube and whose origin can be traced to one of the earlier formed biofilm layers. Under the 'onion model' used to simulate biofilm growth, each antecedent layer must leave no empty space in order for a subsequent layer to begin growing. This effectively constrains growth as laminar. For this simulation, we used $v = 0.0$ and $\mu = 0.0025$, which yielded a total of 18 categorical variants.

ulations. Phenotypic plasticity of genetically uniform individuals is well accepted as an important contributor to the overall phenotypic variance exhibited by biofilm populations (Wiuff *et al.*, 2005; Jothi *et al.*, 2009). Moreover, interactions among organisms within biofilms may be locally intense and the ecological conditions under which resistant phenotypes arise and proliferate may be far from neutral. It is quite possible that the variants that come to persist within biofilms and ultimately confer antimicrobial resistance genetically hitchhike with genes that offer selective advantage under natural conditions of biofilm growth and maturation (e.g. see Wrands *et al.*, 2008). Whether heritable trait variation that arises in biofilms is generally dominated by correlated selection or the accumulation of neutral variation is currently unsettled (e.g. Waite *et al.*, 2001; Boles *et al.*, 2004; Bantinaki *et al.*, 2007; Battin *et al.*, 2007; Yarwood *et al.*, 2007; Boles & Singh, 2008; Ponciano *et al.*, 2009). Involving evolutionary non-neutrality will nevertheless be an important extension to model introduced here. Even if phenotypic

variants differ in global selective value, there is a spatial threshold (i.e. the ecological neighbourhood) beyond which interorganismal interactions will be weak. In an assemblage that can involve billions of cells, such spatial structuring may contribute strongly to the extent of diversity that can be maintained within the biofilm (Gause, 1932; Wright, 1943; see also Hallatschek *et al.*, 2007; Prado & Kerr, 2009; and Hallatschek & Nelson, 2010). Indeed, we find that spatially structured growth drives elevated phenotypic variance in simulation (Fig. 4). Only those variants that are present within (or very near) the growth front have the ability to be propagated. Drift is thus intensified at the edge of growth as emergent layers in the biofilm sample diversity from a relatively small population of progenitors. This pattern appears to be a general feature of any rapidly expanding and spatially structured population (Hallatschek *et al.*, 2007; Excoffier & Nicolas, 2008; Hallatschek & Nelson, 2010).

The role of spatial dependence in growth dynamics is yet to be addressed as a factor involved in the accumulation and distribution of variation within biofilms. Under normal conditions of growth, Ponciano *et al.* (2009) observe a trend towards greater variability in growth kinetics for isolates sampled from the most newly formed layers of a cultured biofilm. In modelling bacterial growth kinetics in biofilms, it further appears that turnover in the deepest layers of the biofilm may occur disproportionately fast. If replicative mutation overwhelmingly contributes to the origin of novel variation, rapid overturn in the earliest layers might imply an early burst of phenotypic diversification within a maturing biofilm. As we find in simulation (see Fig. 4), spatially structured growth exacerbates the extent of diversity that is maintained in biofilms. This may be especially true if growth conditions experienced by a biofilm periodically fluctuate and/or turnover of individuals is non-negligible (Kassen & Rainey, 2004). There may be considerable periods of diversity remodelling and renewal within the biofilm, generated by both replication-dependent and replication-independent processes.

The general finding of elevated phenotypic variation over time (J.G. Tyerman *et al.*, unpublished data) and spatially within *E. coli* biofilms (Ponciano *et al.*, 2009) would suggest that a stochastic process is at least partly responsible in the sorting and preservation of phenotypic variants that emerge in these bacterial communities. The observed increase in phenotypic variation would seem to be well described by a diffusion process, as modelled here, that is free from any directional expectation (e.g. towards generally greater or lesser sensitivity to antimicrobials). In a phenotypically diverse community, the community as a whole has a greater chance of comprising at least some members that are preadapted for novel environmental conditions (i.e. a so-called insurance effect; Yachi & Loreau, 1999; Boles *et al.*, 2004). Whereas more mature biofilms may exhibit no more resistance *on average* than a younger biofilm (see J.G. Tyerman *et al.*, unpublished

data), an elevation in phenotypic variance would imply a greater overall chance of observing at least one *highly* resistant (or sensitive) variant, and this probability may increase in proportion to the duration of the evolutionary process. Our simulations conducted under a simple and neutral evolutionary model (e.g. Fig. 5) suggest that the accumulation of neutral variation may be sufficient to explain observed patterns of phenotypic diversity in real biofilms. Our simulation work appears quite consistent with the stratification of diversity observed in the biofilms investigated by Ponciano *et al.* (2009). For more quantitative comparisons with empirical data, it may be possible to estimate the parameters used in the simulated Moran process (μ and ν) from observed patterns of diversity stratification (e.g. in the vein of Luria & Delbrück, 1943; see Keightley & Bataillon, 2000).

Simulations conducted herein consider biofilms that were fractions of the cell abundances observed for *E. coli* biofilms. Simulations involved biofilms with at most 10^6 cells, many orders of magnitude smaller than the predicted abundance of *in vitro* biofilms. If we assume that individual cells are roughly $0.5 \mu\text{m}$ in diameter and $2 \mu\text{m}$ in length (Holt, 1994), there may be as many as 10^{11} – 10^{12} cells within a mature *in vitro* biofilm of *E. coli* (see Ponciano *et al.*, 2009 for experimental conditions informing this estimate). We have not thoroughly explored the dependence of results upon size of simulated biofilms, but results from simulations conducted with much smaller biofilms (total volume between 10^4 and 10^5 individuals) are qualitatively unchanged. It may be possible to adapt existing methods in the coalescent (e.g. Rosindell *et al.*, 2008) to catalogue the complete genealogy of mutations in ‘samples’ from layers of a biofilm. This reverse-time approach would enable simulations involving more realistic population sizes (e.g. billions of individuals rather than millions, as is currently) while also considering realistic sample sizes.

Conclusions

The predictive patterns of diversity structuring that arise through these simulations consistently and considerably differ from those expected where the mechanism of resistance does not involve considerable contributions from heritable variation. Much as J.G. Tyerman *et al.* (unpublished data) propose as a potential explanation for antibiotic resistance in the absence of selection for resistance, we find that under a simple ‘onion model’ of growth and mutation, heritable variation can indeed accumulate through strata of the biofilm. Results presented here should aid future work in assessing the relative contribution of mutational processes in the spatial distribution and overall extent of diversity within biofilms. We argue that a richer understanding of antimicrobial resistance in biofilm populations will likely involve an evolutionary context.

Acknowledgments

The project benefited from numerous conversations with Ana Cornea and James Rosindell. We wish to thank Olivier Tenaillon and an anonymous reviewer for offering constructive comments and important corrections on a previous version of the manuscript. Financial support to LJH was provided by NSF DEB 0919499 and the BEACON Center for the Study of Evolution in Action (NSF DBI0939454), and to LJJ from an NIH Center of Biomedical Research Excellence grant (P2ORR16448-07S2) from the National Center for Research Resources, and a grant from Proctor & Gamble.

References

- Balaban, N.O., Merrin, J., Chait, R., Kowalik, L. & Leibler, S. 2004. Bacterial persistence as a phenotypic switch. *Science* **305**: 1622–1625.
- Bantinaki, E., Kassen, R., Knight, C., Robinson, Z., Spiers, A.J. & Rainey, P.B. 2007. Adaptive divergence in experimental populations of *Pseudomonas fluorescens* III. Mutational origins of wrinkly spreader diversity. *Genetics* **176**: 441–453.
- Battin, T.J., Sloan, W.T., Kjelleberg, S., Daims, H., Head, I.M., Curtis, T.P. *et al.* 2007. Microbial landscapes: new paths to biofilm research. *Nat. Rev. Microbiol.* **5**: 76–81.
- Bjedov, I., Tenaillon, O., Gerard, B., Souza, V., Denamur, E., Radman, M. *et al.* 2003. Stress-induced mutagenesis in bacteria. *Science* **300**: 1404–1409.
- Boles, B.R. & Singh, P.K. 2008. Endogenous oxidative stress produces diversity and adaptability in biofilm communities. *Proc. Natl Acad. Sci. USA* **105**: 12503–12508.
- Boles, B.R., Thoendel, M. & Singh, P.K. 2004. Self-generated diversity produces “insurance effects” in biofilm communities. *PNAS* **101**: 16630–16635.
- Chang, I., Gilbert, E.S., Eliashberg, N. & Keasling, J.D. 2003. A three-dimensional, stochastic simulation of biofilm growth and transport-related factors that affect structure. *Microbiology* **149**: 2859–2871.
- Charlesworth, B. 2009. Fundamental concepts in genetics: effective population size and patterns of molecular evolution and variation. *Nat. Rev. Gen.* **10**: 195–205.
- Chen, X. & Stewart, P.S. 1996. Chlorine penetration into artificial biofilm is limited by a reaction–diffusion interaction. *Environ. Sci. Technol.* **30**: 2078–2083.
- Cochran, W.L., McFeters, G.A. & Stewart, P.S. 2000. Reduced susceptibility of thin *Pseudomonas aeruginosa* biofilms to hydrogen peroxide and monochloramine. *J. Appl. Microbiol.* **88**: 22–30.
- Conibear, T.C., Collins, S.L. & Webb, J.S. 2009. Role of mutation in *Pseudomonas aeruginosa* biofilm development. *PLoS ONE* **14**: e6289.
- Costerton, J.W., Cheng, K.-J., Geesey, G.G., Ladd, T.I., Nickel, J.C., Dasgupta, M. *et al.* 1987. Bacterial biofilms in nature and disease. *Annu. Rev. Microbiol.* **41**: 435–464.
- Drenkard, E. & Ausubel, F.M. 2002. *Pseudomonas* biofilm formation and antibiotic resistance are linked to phenotypic variation. *Nature* **416**: 740–743.

- Excoffier, L. & Nicolas, R. 2008. Surfing during population expansions promotes genetic revolutions and structuration. *Trends Ecol. Evol.* **23**: 347–351.
- Felsenstein, J. 1973. Maximum-likelihood estimation of evolutionary trees from continuous characters. *Am. J. Hum. Genet.* **25**: 471–492.
- Galhardo, R.S., Hastings, P.J. & Rosenberg, S.M. 2007. Mutation as a stress response and the regulation of evolvability. *Crit. Rev. Biochem. Mol. Biol.* **42**: 399–435.
- Gause, G.F. 1932. Experimental studies on the struggle for existence: 1. Mixed population of two species of yeast. *J. Exp. Biol.* **9**: 389–402.
- Gini, C. 1912. *Variabilità e Mutabilità (Variability and Mutability)*. C. Cuppini, Bologna.
- Hallatschek, O. & Nelson, D.R. 2010. Life at the front of an expanding population. *Evolution* **64**: 193–206.
- Hallatschek, O., Hersen, P., Ramanathan, S. & Nelson, D.R. 2007. Genetic drift at expanding frontiers promotes gene segregation. *Proc. Natl Acad. Sci. USA* **104**: 19926–19930.
- Hall-Stoodley, L., Costerton, J.W. & Stoodley, P. 2004. Bacterial biofilms: from the natural environment to infectious diseases. *Nat. Rev. Microbiol.* **2**: 95–108.
- Holt, J.G. 1994. *Bergey's Manual of Determinative Bacteriology*, 9th edn. Williams and Wilkins, Baltimore, MD.
- Jothi, R., Balaji, S., Wuster, A., Grochow, J.A., Gsponer, J., Przytycka, T.M. et al. 2009. Genomic analysis shows a tight link between transcription factor dynamics and regulatory network architecture. *Mol. Syst. Biol.* **5**: 294.
- Kassen, R. & Rainey, P.B. 2004. The ecology and genetics of microbial diversity. *Annu. Rev. Microbiol.* **58**: 207–231.
- Keightley, P.D. & Bataillon, T.M. 2000. Multigeneration maximum-likelihood analysis applied to mutation-accumulation experiments in *Caenorhabditis elegans*. *Genetics* **154**: 1193–1201.
- Kimura, M. 1983. *The Neutral Theory of Molecular Evolution*. Cambridge University Press, Cambridge, MA.
- Kimura, M. & Crow, J. 1964. The number of alleles that can be maintained in a finite population. *Genetics* **49**: 725–738.
- Kingman, J.F.C. 1982. On the genealogy of large populations. *J. Appl. Prob.* **19A**: 27–43.
- Kreft, J.-U., Booth, G. & Wimpenny, J.W.T. 1998. Bacsim, a simulator for individual-based modelling of bacterial colony growth. *Microbiology* **144**: 3275–3287.
- Lewis, K. 2001. Riddle of biofilm resistance. *Antimicrob. Agents Chemother.* **45**: 999–1007.
- Luria, S.E. & Delbrück, M. 1943. Mutations of bacteria from virus sensitivity to virus resistance. *Genetics* **28**: 491–511.
- Mah, T.F. & O'Toole, G.A. 2001. Mechanisms of biofilm resistance to antimicrobial agents. *Trends Microbiol.* **9**: 34–39.
- Matic, I., Radman, M., Taddei, F., Picard, B., Dolt, C., Bingen, E. et al. 1997. Highly variable mutation rates in commensal and pathogenic *Escherichia coli*. *Science* **277**: 1833–1834.
- Moran, P.A.P. 1962. *The Statistical Processes of Evolutionary Theory*. Clarendon Press, Oxford.
- Ponciano, J.M., La, H.-J., Joyce, P. & Forney, L.J. 2009. Evolution of diversity in spatially structured *Escherichia coli* populations. *Appl. Environ. Microbiol.* **75**: 6047–6054.
- Prado, F. & Kerr, B. 2009. The evolution of restraint in bacterial biofilms under nontransitive competition. *Evolution* **62**: 538–548.
- R Development Core Team 2011. *R: A Language and Environment for Statistical Computing*. R Foundation for Statistical Computing, Vienna, Austria, ISBN 3-900051-07-0, Available from <http://www.R-project.org>.
- Rosindell, J., Wong, Y. & Etienne, R.S. 2008. A coalescent approach in spatial neutral ecology. *Ecol. Inform.* **2008**: 259–271.
- Simpson, E.H. 1949. Measurement of diversity. *Nature* **163**: 688.
- Stewart, P.S. 1996. Theoretical aspects of antibiotic diffusion into microbial biofilms. *Antimicrob. Agents Chemother.* **40**: 2517–2522.
- Stewart, P.S. & Costerton, J.W. 2001. Antibiotic resistance of bacteria in biofilms. *Lancet* **358**: 135–138.
- Surdeau, N., Laurent-Maquin, D., Bouthors, S. & Gellé, M.P. 2010. Sensitivity of bacterial biofilms and planktonic cells to a new antimicrobial agent, Oxsil® 320N. *J. Hosp. Infect.* **62**: 487–493.
- Waite, R.D., Struthers, J.K. & Dowson, C.G. 2001. Spontaneous sequence duplication within an open reading frame of the pneumococcal type 3 capsule locus causes high frequency phase variation. *Mol. Microbiol.* **42**: 1223–1232.
- Wiuff, C., Zappala, R.M., Regoes, R.R., Garner, K.N., Baquero, F. & Levin, B.R. 2005. Phenotypic tolerance: antibiotic enrichment of noninherited resistance in bacterial populations. *Antimicrob. Agents Chemother.* **49**: 1483–1494.
- Wrande, M., Roth, J.R. & Hughes, D. 2008. Accumulation of mutants in “aging” bacterial colonies is due to growth under selection, not stress-induced mutagenesis. *Proc. Natl Acad. Sci. USA* **105**: 11863–11868.
- Wright, S. 1931. Evolution in Mendelian populations. *Genetics* **16**: 97–159.
- Wright, S. 1943. Isolation by distance. *Genetics* **28**: 114–138.
- Yachi, S. & Loreau, M. 1999. Biodiversity and ecosystem productivity in a fluctuating environment: the insurance hypothesis. *Proc. Natl Acad. Sci. U S A* **96**: 1463–1468.
- Yarwood, J.M., Paquette, K.M., Tikh, I.B., Volper, E.M. & Greenberg, E.P. 2007. Generation of virulence factor variants in *Staphylococcus aureus* biofilms. *J. Bacteriol.* **189**: 7961–7967.

Supporting information

Additional Supporting Information may be found in the online version of this article:

Appendix S1 Results from individual simulations, for two measures of phenotypic diversity.

Appendix S2 Results from simulations under two forms of growth structure: biofilm development (as per the onion model) or ‘planktonic’ culture, modelling diversification in a well-mixed (spatially unstructured) population.

As a service to our authors and readers, this journal provides supporting information supplied by the authors. Such materials are peer-reviewed and may be re-organized for online delivery, but are not copy-edited or typeset. Technical support issues arising from supporting information (other than missing files) should be addressed to the authors.

Received 2 May 2011; revised 28 July 2011; accepted 31 July 2011